Supplemental Figure S1

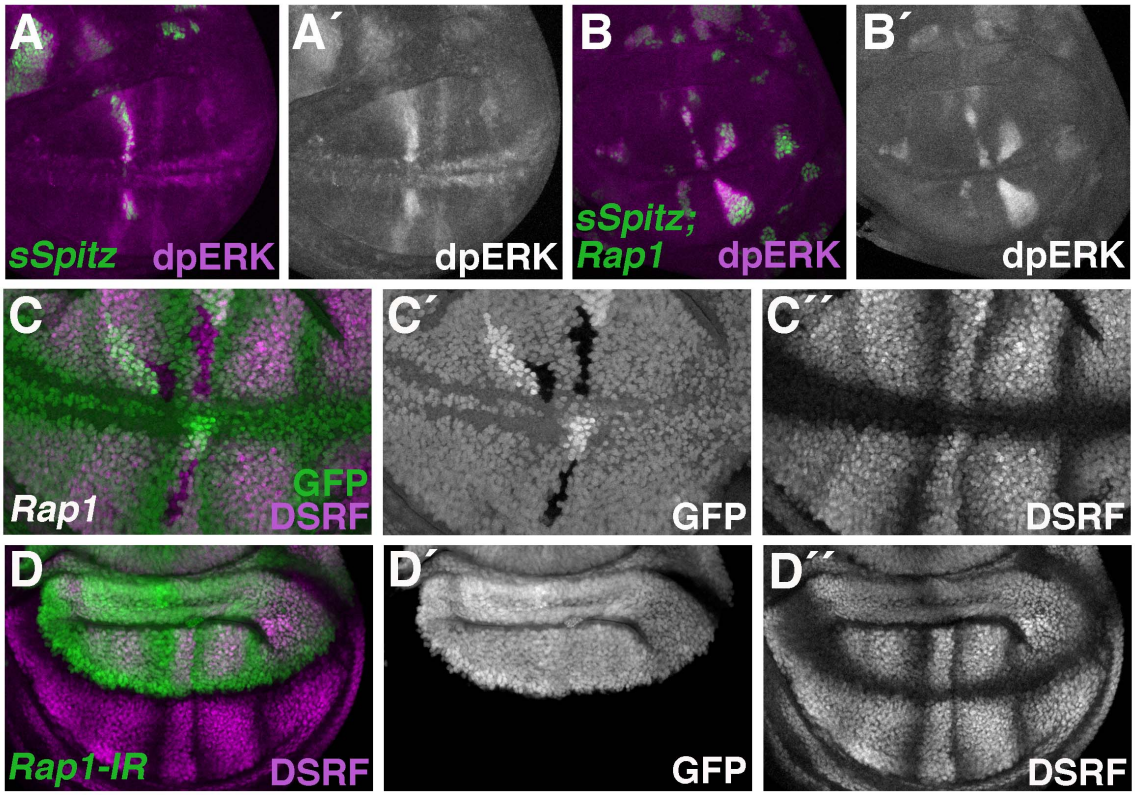

Supplemental Figure S1. Rap1 does not affect Spitz activation of MAPK (ERK) or vein cell specification. (A,B) The MARCM system was used to express a secreted version of Spitz (sSpitz) in wildtype (A) or *Rap1* mutant cells (B). Wing discs stained for dpERK are shown. (A) sSpitz expressing cells (GFP-positive) have elevated levels of dpERK staining. (B) Loss of Rap1 does not affect the ability of sSpitz to elevate dpERK levels. (C) The *Flp/FRT* system was used to generate clones of cells mutant for *Rap1* (GFP-negative) in larval wing discs. DSRF localization is not affected by loss of Rap1. (D) *apterous-Gal4* was used to express *Rap1-IR* in the dorsal compartment of the wing imaginal disc (GFP-positive). DSRF localization is not affected by *Rap1-IR* expression.

Supplemental Figure S2

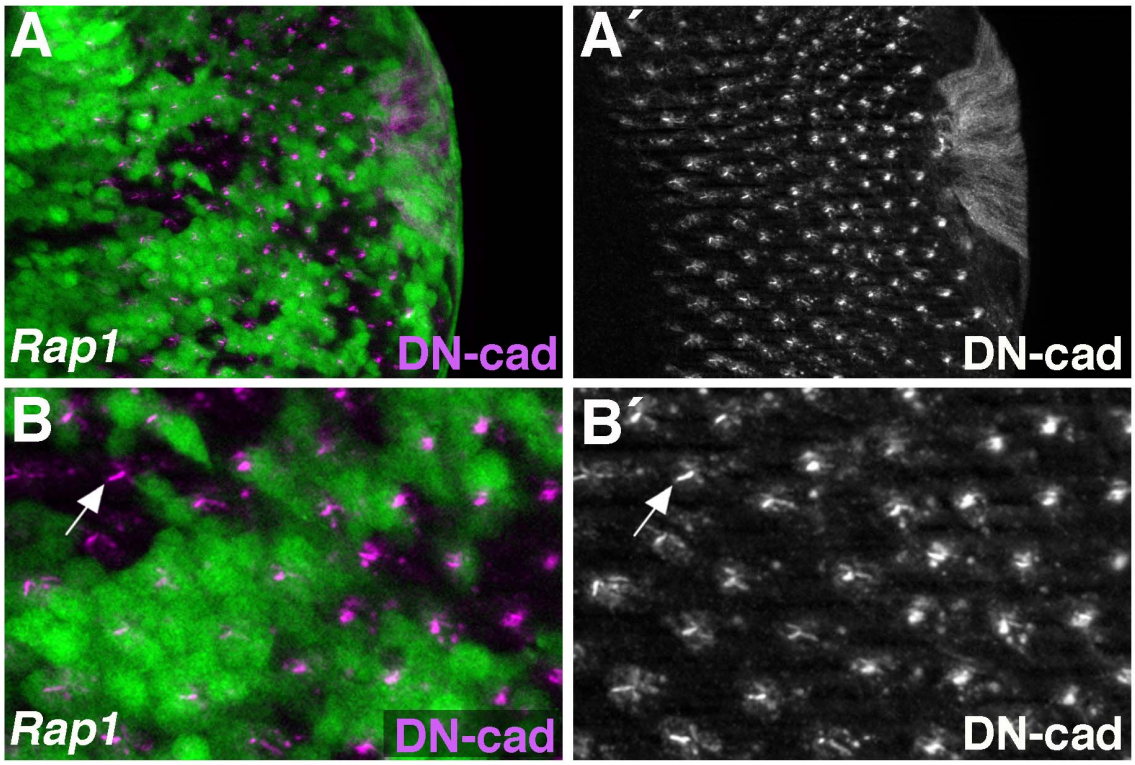

Supplemental Figure S2. Rap1 does not affect DN-cadherin localization in the eye. Clones of cells lacking *Rap1* (GFP-negative) were generated using the ey-*flp*/*FRT* system. Eye imaginal discs were stained for DN-cad. (A) DN-cad localization is unaffected in *Rap1* mutant tissue. (B) Magnified view of A is shown. Arrow indicates *Rap1* mutant precluster with the wildtype pattern of DN-cad localization (highest levels at the R3/R4 cell junction).

Supplemental Figure S3

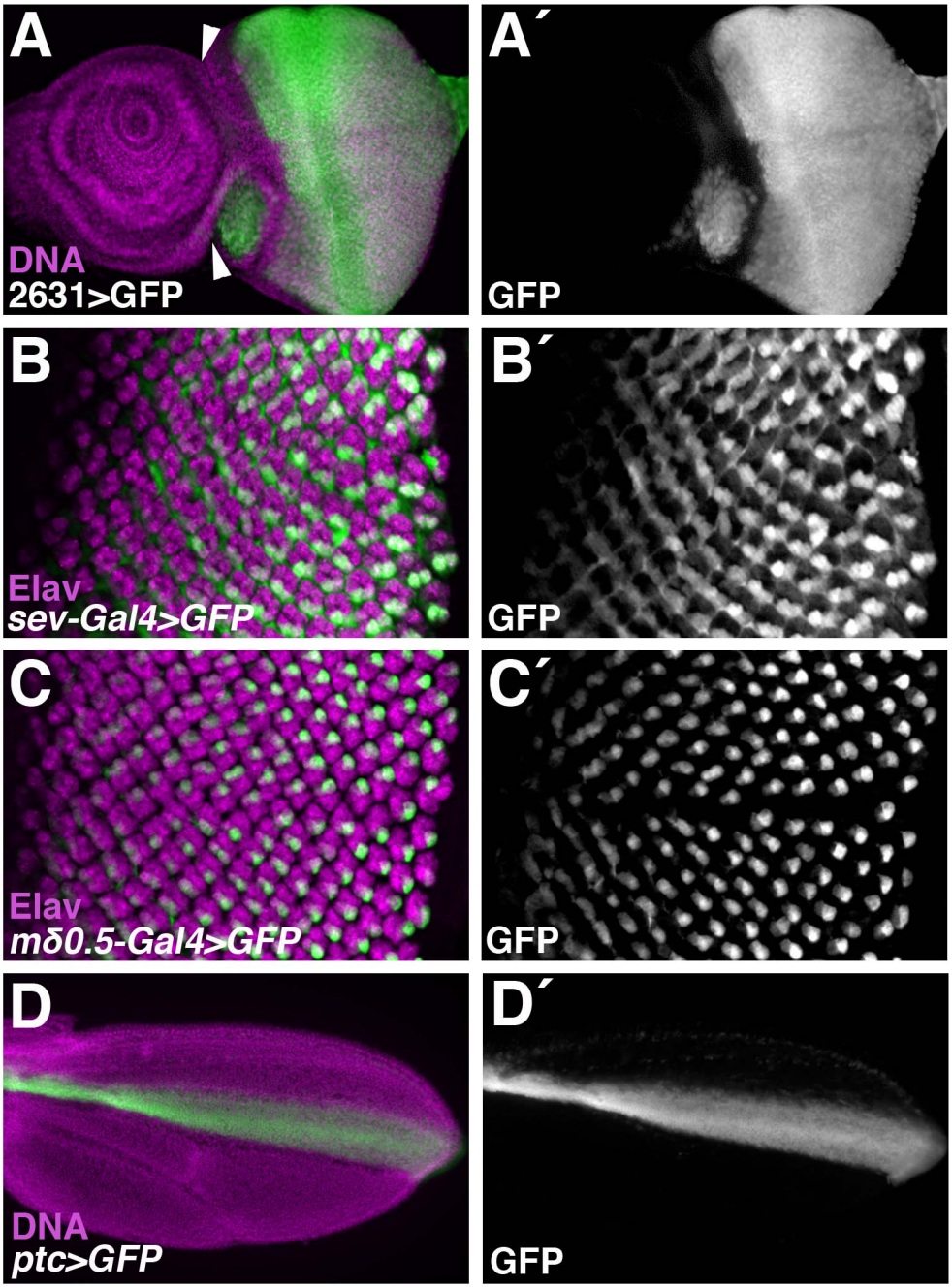

Supplemental Figure S3. Gal4 expression patterns. Gal4 lines were used to drive expression of a UAS-GFP transgene. (A-C) Late third instar eye-antennal discs stained for DNA (A) or Elav (B,C) are shown. *NP2631-Gal4* drives GFP expression in most cells of the eye disc. Arrowheads indicate junction between eye and antennal portions of the disc (antenna to the left). (B) *sev-Gal4* drives expression in a subset of photoreceptor

precursors (R3, R4, and R7) and cone cells. (C) *mδ0.5-Gal4* is expressed at highest levels in R4, but also more weakly in R3 and R7. (D) Pupal wing (36 hours APF) stained for DNA is shown. *ptc-Gal4* drives GFP expression in a stripe of cells between veins L3 and L4.

Supplemental Figure S4

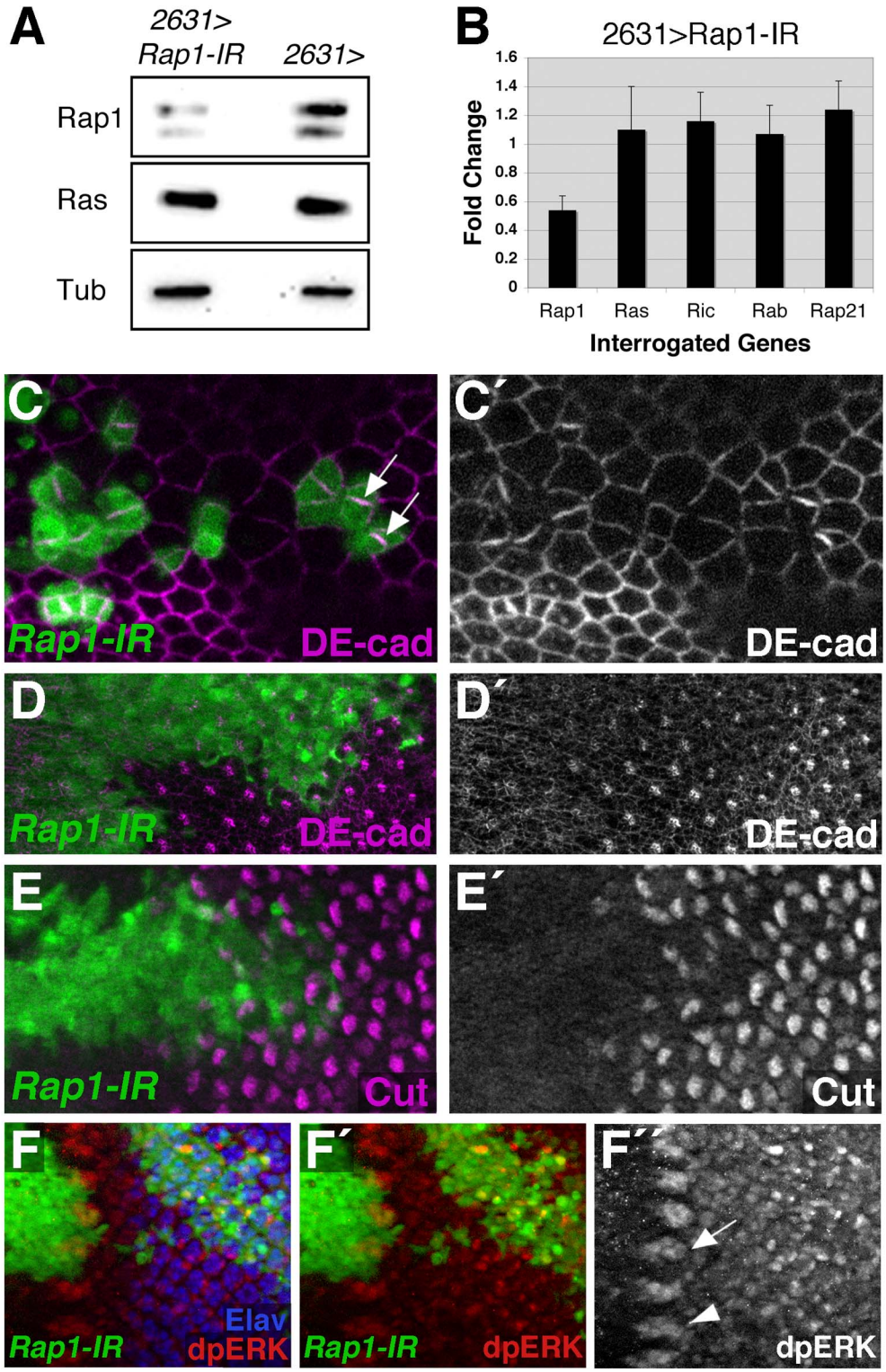

Supplemental Figure S4. *Rap1-IR* controls. (A) Western analysis on control and *NP2631>Rap1-IR* eye discs indicates that Rap1 protein is downregulated, but Ras is

unaffected. (B) qPCR analysis on *NP2631>Rap1-IR* eye discs indicates that *Rap1* expression is downregulated, but other related GTPases are unaffected. (C-F) The *FRT/Gal4* system was used to express *Rap1-IR* in clones of cells (GFP-positive). (A) Pupal wings (36 hour APF), or eye imaginal discs (D-F) are shown. (A) *Rap1-IR* expressing cells exhibit cell shape and DE-cad mislocalization phenotypes similar to *Rap1* loss of function. Arrows indicate high levels of DE-cad found at the interface between two *Rap1-IR* expressing cells. *Rap1-IR* expression results in lower levels of DE-cad (D) and loss of Cut-positive cone cells (E) as seen with *Rap1* loss of function. (F) *Rap1-IR* expression does not affect dpERK localization. Arrow and arrowhead indicate *Rap1-IR*-expressing and wildtype ommatidia respectively.

Supplemental Figure S5

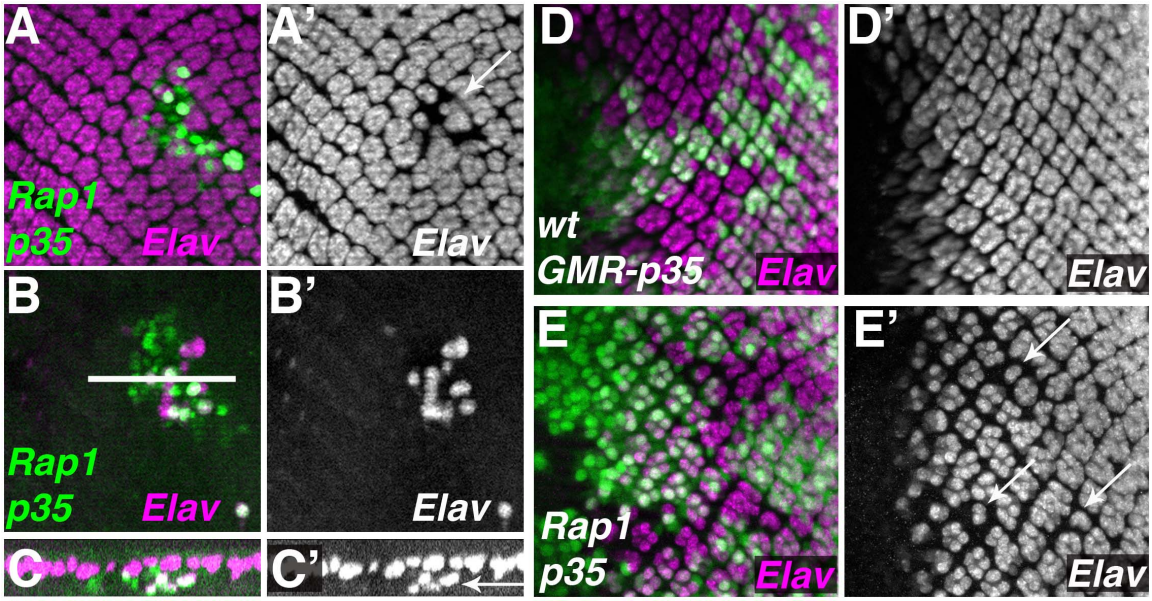

Supplemental Figure S5. The apoptosis inhibitor p35 does not prevent the effects of *Rap1* mutant clones on photoreceptor development. (A-C) The MARCM system was used to express the Caspase inhibitor p35 in *Rap1* mutant cells. (D,E) The *Flp/FRT* system and an *eyflp* transgene were used to generate wild-type (D) and *Rap1*- (E) clones in eye discs expressing p35 behind the furrow under control of the GMR enhancer. (A) Projection of multiple optical sections encompassing all Elav-stained nuclei. (B) Single basal sections of the disc shown in (A). (C) Cross-section of the disc shown in (A,B); position of the cross-section denoted by a white line in B. Elav-expressing nuclei in and adjacent to *Rap1* mutant clones are found basally. (D) Expression of p35 in cells behind the furrow has no discernible effect on photoreceptor development during larval stages. (E) *Rap1*- clones show a loss of photoreceptors even in the presence of p35.

Supplemental Figure S6

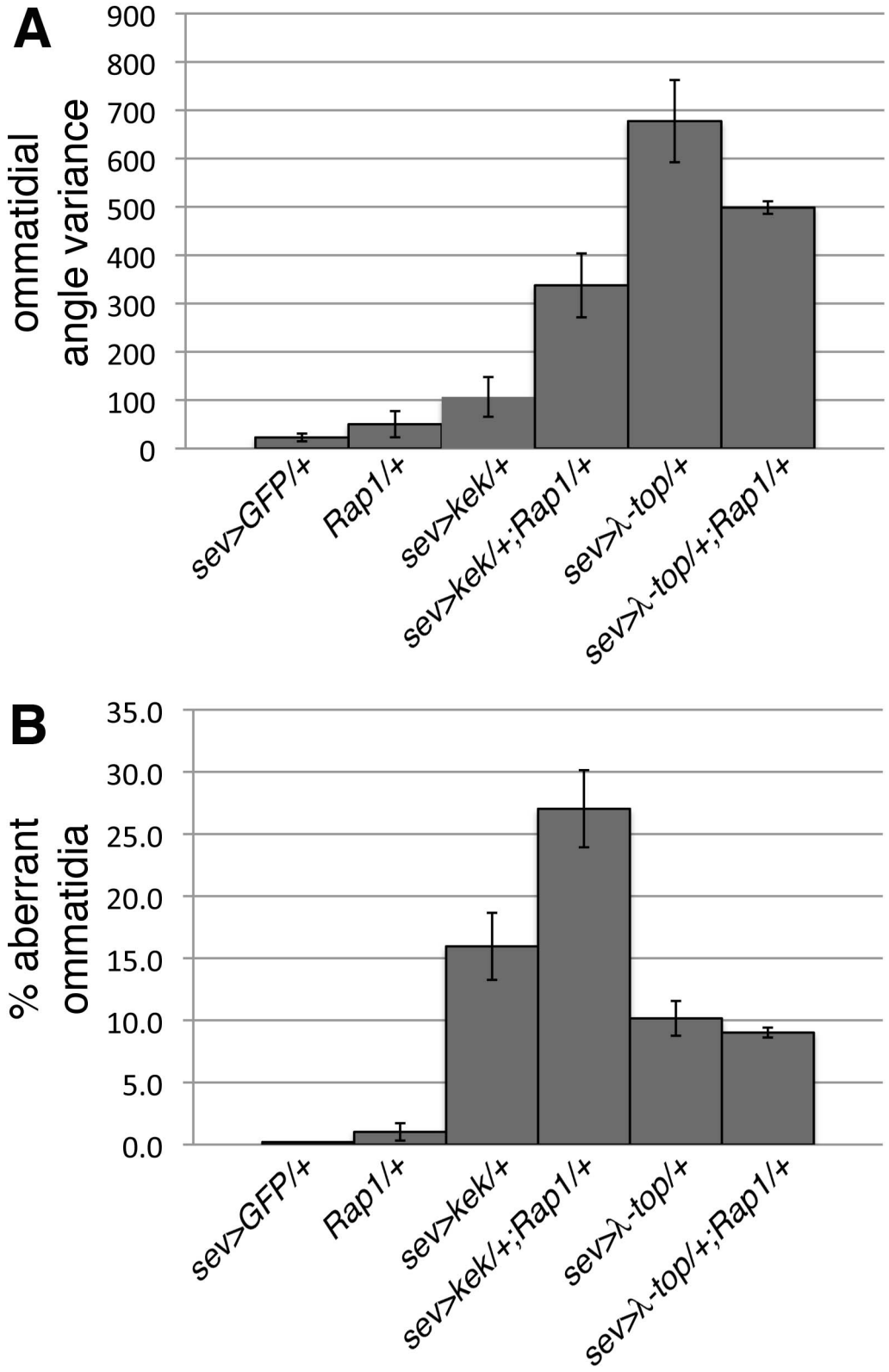

Supplemental Figure S6. *Rap1-* mutations modify ommatidial rotation defects and photoreceptor loss/gain caused by reduction or gain of Egfr pathway activity. Quantifications of *Rap1* genetic interactions with *sev-kek* and *sev-λ-top* are shown. Loss of one copy of *Rap1* significantly increases ommatidial misalignment and the percentage of aberrant ommatidia associated with *sev-kek* heterozygotes ($p<0.05$). Conversely, loss of *Rap1* significantly decreases the same defects associated with *sev-λ-top* heterozygotes ($p<0.05$).

Supplemental Figure S7

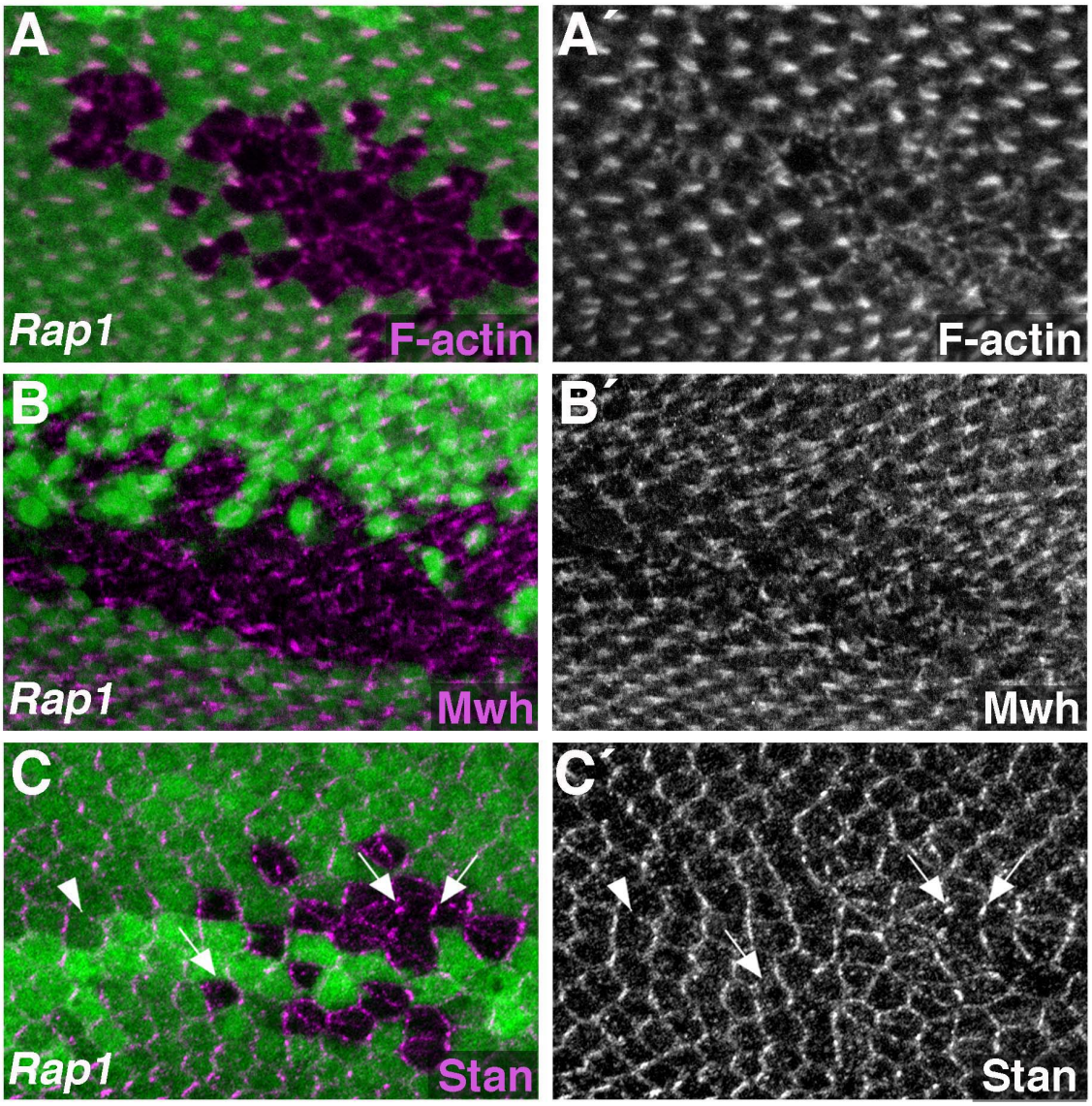

Supplemental Figure S7. Localization of polarized proteins in *Rap1* mutant wing cells. (A-C) The *Flp/FRT* system was used to generate *Rap1* mutant clones of cells (GFP-negative). Pupal wings (32 hour APF) were stained for F-actin (A), Mwh (B), or Stan (C). (A) In *Rap1* mutant cells, F-actin no longer localizes to a single pre-hair. (B) Mwh localization is abnormal in *Rap1* mutant cells. Mwh and F-actin are similarly mislocalized in *Rap1* mutant cells (compare A and B). (C) In wildtype wing cells, Stan is concentrated at the proximal/distal edges of each cell. Arrowhead indicates low levels of Stan at anterior/posterior edges of wildtype cells. In *Rap1* mutant cells, high levels of

Stan concentrated at proximal/distal cell edges are still observed (arrows), indicating that Rap1 does not significantly affect Stan localization.